



Wideband microwave phase noise measurement based on photonic-assisted I/Q mixing and digital phase demodulation

FANGZHENG ZHANG, JINGZHAN SHI, AND SHILONG PAN*

Key Laboratory of Radar Imaging and Microwave Photonics, Ministry of Education, Nanjing University of Aeronautics and Astronautics, Nanjing 210016, China

*pans@ieee.org

Abstract: A wideband microwave phase noise measurement system is proposed based on quadrature phase demodulation of the mixing components of a signal under test (SUT) and its delayed replica. The time delay is introduced by a low-loss optical fiber, which can be sufficiently large to achieve a high phase noise measurement sensitivity, and the quadrature phase demodulation is achieved by photonic-assisted in-phase and quadrature (I/Q) mixing together with digital signal processing. Thanks to the optoelectronic hybrid quadrature phase demodulation, the use of feedback loops, which are usually required in conventional photonic-delay-line-based phase noise measurement systems, is avoided, and the measurable frequency range is expanded. An experiment is implemented. Accurate phase noise measurement of SUTs in a frequency range of 5-35 GHz is demonstrated. With a 2-km single-mode fiber serving as the photonic delay line, the phase noise floor is as low as -131 dBc/Hz at the offset frequency of 10 kHz. The proposed scheme can be applied for evaluating the performance of microwave systems using low-phase-noise and wideband tunable microwave sources.

© 2017 Optical Society of America

OCIS codes: (060.5625) Radio frequency photonics; (120.0120) Instrumentation, measurement, and metrology; (060.4080) Modulation.

References and links

1. D. B. Leeson, "Oscillator phase noise: a 50-year review," *IEEE Trans. Ultrason. Ferroelectr. Freq. Control* **63**(8), 1208–1225 (2016).
2. A. K. Poddar, U. L. Rohde, and A. M. Apte, "How low can they go?: oscillator phase noise model, theoretical, experimental validation, and phase noise measurements," *IEEE Microw. Mag.* **14**(6), 50–72 (2013).
3. U. L. Rohde, A. K. Poddar, and A. M. Apte, "Getting its measure: oscillator phase noise measurement techniques and limitations," *IEEE Microw. Mag.* **14**(6), 73–86 (2013).
4. E. Rubiola, E. Salik, S. Huang, N. Yu, and L. Maleki, "Photonic-delay technique for phase-noise measurement of microwave oscillators," *J. Opt. Soc. Am. B* **22**(5), 987–997 (2005).
5. B. Onillon, S. Constant, and O. Liopis, "Optical links for ultra-low phase noise microwave oscillators measurement," in *IEEE International Frequency Control Symposium and Exposition*, 545–550, (2005).
6. P. Salzenstein, E. Pavlyuchenko, A. Hmima, N. Cholley, M. Zarubin, S. Galliou, Y. Chembo, and L. Larger, "Estimation of the uncertainty for a phase noise optoelectronic metrology system," *Phys. Scr. T* **149**, 014025 (2012).
7. S. Pan and J. Yao, "Photonics-based broadband microwave measurement," *J. Lightwave Technol.* **35**(16), 3498–3513 (2017).
8. D. Zhu, F. Zhang, P. Zhou, D. Zhu, and S. Pan, "Wideband phase noise measurement using a multifunctional microwave photonic processor," *IEEE Photonics Technol. Lett.* **26**(24), 2434–2437 (2014).
9. W. Wang, J. Liu, H. Mei, W. Sun, and N. Zhu, "Photonic-assisted wideband phase noise analyzer based on optoelectronic hybrid units," *J. Lightwave Technol.* **34**(14), 3425–3431 (2016).
10. D. Zhu, F. Zhang, P. Zhou, and S. Pan, "Phase noise measurement of wideband microwave sources based on a microwave photonic frequency down-converter," *Opt. Lett.* **40**(7), 1326–1329 (2015).
11. F. Zhang, D. Zhu, and S. Pan, "Photonic-assisted wideband phase noise measurement of microwave signal sources," *Electron. Lett.* **51**(16), 1272–1274 (2015).
12. S. O. Tatu, E. Moldovan, S. Affes, B. Boukari, K. Wu, and R. G. Bosisio, "Six-port interferometric technique for accurate W-band phase-noise measurements," *IEEE Trans. Microw. Theory Tech.* **56**(6), 1372–1379 (2008).
13. H. Gheidi and A. Banai, "Phase-noise measurement of microwave oscillators using phase-shifterless delay line discriminator," *IEEE Trans. Microw. Theory Tech.* **58**(2), 468–477 (2010).

14. K. Volyanskiy, J. Cussey, H. Tavernier, P. Salzenstein, G. Sauvage, L. Larger, and E. Rubiola, "Applications of the optical fiber to the generation and measurement of low-phase-noise microwave signals," *J. Opt. Soc. Am. B* **25**(12), 2140–2150 (2008).
15. E8257D PSG Microwave Analog Signal Generator Data Sheet, Keysight Technologies Co. USA, 17–20 (2016).

1. Introduction

Phase noise is an important parameter for evaluating the short-term frequency stability of a microwave signal source in communication, radar and other systems [1]. With the rapid development of low phase noise and wideband-tunable microwave signal sources, accurate phase noise characterization of signals in a large frequency range is becoming increasingly important [2,3]. Photonic-delay-line-based phase noise measurement, which acquires the phase noise by mixing the signal under test (SUT) with its optically delayed replica, attracts great attentions thanks to its high phase noise measurement sensitivity [4–7]. To measure the phase noise of signals in a large frequency range, the bandwidth limitation of electrical phase shifters and frequency mixers should be overcome, which can be solved by implementing microwave phase shifting and frequency mixing in the optical domain [8–11]. However, a feedback loop is required in these systems to ensure that the SUT and its delayed copy are quadrature to each other before sent to a frequency mixer, which is usually implemented by dynamically controlling an adjustable electrical or microwave photonic phase shifter incorporated in the feedback loop. The use of a feedback loop would not only result in a complicated system structure, but also cause measurement error by affecting the phase noise within the locking bandwidth of the feedback loop. One promising method to eliminate the use of the feedback loop and the tunable phase shifter is to apply quadrature phase demodulation, in which the phase information is acquired from the in-phase and quadrature (I/Q) components of the signal [12,13]. However, in the previously-reported electrical phase noise measurement systems based on quadrature phase demonstration, two parallel electronic frequency mixers are required to achieve the in-phase and quadrature mixing components, which could easily induce I/Q mismatch and thus affect the measurement accuracy. In addition, the measurement sensitivity and the frequency range are restricted by the large loss electrical delay line and multiple electrical frequency mixers.

In this paper, we propose and investigate a novel photonic-delay-line-based microwave phase noise measurement system based on photonic-assisted I/Q mixing and digital phase demodulation. Because feedback loops and tunable phase shifters are not required, the proposed system is simple and compact. In addition, thanks to the use of low-loss optical fiber as the photonic delay line, a large amount of time delay can be introduced, leading to a high phase noise measurement sensitivity. The system also has a large measurement frequency range since the photonic-assisted I/Q mixing is intrinsically broadband. An experiment is carried out. A phase noise measurement system is established with its measurement accuracy, measurement sensitivity and measurement frequency range tested.

2. Operation principle

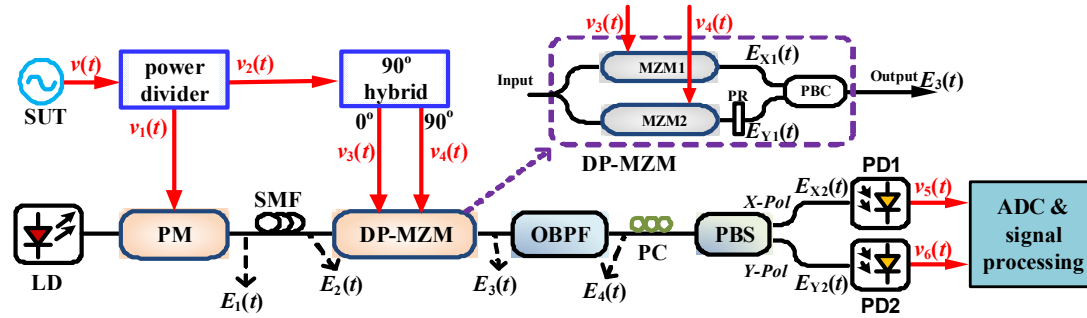


Fig. 1. Schematic diagram of the proposed phase noise measurement system. SUT: signal under test; LD: laser diode; PM: phase modulator; SMF: single mode fiber; DP-MZM: dual-polarization Mach-Zehnder beam modulator; PR: polarization rotator; PBC: polarization beam combiner; OBPF: optical band-pass filter; PC: polarization controller; PBS: polarization beam splitter; PD: photodetector; ADC: analog-to-digital converter.

Figure 1 shows the schematic diagram of the proposed phase noise measurement system. The SUT is assumed to be

$$v(t) = [V_0 + \varepsilon(t)] \cos[\omega_s t + \varphi(t)]. \quad (1)$$

where V_0 and ω_s are the amplitude and angular frequency of the SUT, and $\varepsilon(t)$ and $\varphi(t)$ are the amplitude and phase fluctuations, respectively. The SUT is divided into two branches by a power divider to obtain two identical signals, i.e., $v_1(t)$ and $v_2(t)$. A continuous wave (CW) light from a laser diode (LD) is modulated by a phase modulator (PM) that is driven by signal $v_1(t)$. The optical field after phase modulation is

$$E_1(t) = E_0 \cos\{\omega_c t + \beta \cos[\omega_s t + \varphi(t)]\}. \quad (2)$$

where E_0 and ω_c is the amplitude the angular frequency of the optical carrier, respectively, and β is the phase modulation index. When this optical signal passes through a span of single mode fiber (SMF), the delayed optical signal is

$$E_2(t) = E_0 \cos\{\omega_c(t - \tau) + \beta \cos[\omega_s(t - \tau) + \varphi(t - \tau)]\}. \quad (3)$$

where τ is the time delay due to the SMF. The optical signal from the SMF is sent to a dual-polarization Mach-Zehnder modulator (DP-MZM), which consists of two sub-MZMs (MZM1 and MZM2), a polarization rotator (PR), and a polarization beam combiner (PBC), as shown in the dashed box in Fig. 1. At the same time, two electrical signals, denoted by $v_3(t)$ and $v_4(t)$, are obtained by passing signal $v_2(t)$ through a 90° hybrid. The two signals have a 90° phase difference, and they can be expressed as

$$\begin{aligned} v_3(t) &= \frac{1}{2} [V_0 + \varepsilon(t)] \cos[\omega_s t + \varphi(t)]. \\ v_4(t) &= \frac{1}{2} [V_0 + \varepsilon(t)] \sin[\omega_s t + \varphi(t)]. \end{aligned} \quad (4)$$

Signal $v_3(t)$ and signal $v_4(t)$ are used to drive MZM1 and MZM2, respectively, and the two sub-MZMs are both biased at the quadrature point. In this case, at the output of the DP-MZM, a polarization multiplexed optical signal is obtained given by

$$\begin{aligned}
E_3(t) &= \hat{x}E_{x1}(t) + \hat{y}E_{y1}(t) \\
&= \hat{x} \left\{ E_2(t) \cdot \cos \left[\alpha \cos(\omega_s t + \varphi(t)) + \frac{\pi}{4} \right] \right\} \\
&\quad + \hat{y} \left\{ E_2(t) \cdot \cos \left[\alpha \sin(\omega_s t + \varphi(t)) + \frac{\pi}{4} \right] \right\}.
\end{aligned} \tag{5}$$

where $\alpha = \pi[V_0 + \varepsilon(t)]/4V_\pi$ is the modulation index of each sub-MZM with V_π being the half-wave voltage. The two stages of electro-optical modulations at the PM and the DP-MZM can produce two +1st-order sidebands and two -1st-order sidebands in x and y polarizations, respectively. After the DP-MZM, an optical band-pass filter (OBPF) is used to select out the +1st-order sidebands or the -1st-order sidebands. Based on Jacobi-Anger expansions, the optical signal when selecting out the -1st-order sidebands is calculated to be

$$\begin{aligned}
E_4(t) &= \hat{x}E_{x2}(t) + \hat{y}E_{y2}(t) \\
&= \hat{x} \frac{-\sqrt{2}}{2} E_0 \left\{ \begin{aligned} &J_0(\beta)J_1(\alpha) \cos[(\omega_c - \omega_s)(t - \tau) - \omega_s \tau - \varphi(t)] \\ &+ J_0(\alpha)J_1(\beta) \sin[(\omega_c - \omega_s)(t - \tau) - \varphi(t - \tau)] \end{aligned} \right\} \\
&\quad + \hat{y} \frac{-\sqrt{2}}{2} E_0 \left\{ \begin{aligned} &-J_0(\beta)J_1(\alpha) \sin[(\omega_c - \omega_s)(t - \tau) - \omega_s \tau - \varphi(t)] \\ &+ J_0(\alpha)J_1(\beta) \sin[(\omega_c - \omega_s)(t - \tau) - \varphi(t - \tau)] \end{aligned} \right\}.
\end{aligned} \tag{6}$$

where $J_n(\bullet)$ denotes the n^{th} -order Bessel function of the first kind. Then, the signals in different polarizations are separated using a polarization controller (PC) and a polarization beam splitter (PBS). The two separated optical signals (E_{x2} and E_{y2}) are converted into electrical domain, respectively, at two photodetectors (PD1 and PD2). The voltages of the generated two electrical signals are

$$\begin{aligned}
v_5(t) &= RZ_L |E_{x2}|^2 = V_{DC} + Q(t). \\
v_6(t) &= RZ_L |E_{y2}|^2 = V_{DC} + I(t).
\end{aligned} \tag{7}$$

where R is the responsivity of PD1 and PD2, and Z_L is the input impedance. In (7), V_{DC} , $Q(t)$ and $I(t)$ are given by

$$\begin{aligned}
V_{DC} &= \frac{E_0^2 R Z_L}{4} [J_0^2(\beta)J_1^2(\alpha) + J_0^2(\alpha)J_1^2(\beta)]. \\
Q(t) &= \frac{E_0^2 R Z_L J_0(\beta)J_1(\alpha)J_0(\alpha)J_1(\beta)}{2} \sin[\omega_s \tau + \varphi(t) - \varphi(t - \tau)]. \\
I(t) &= \frac{E_0^2 R Z_L J_0(\beta)J_1(\alpha)J_0(\alpha)J_1(\beta)}{2} \cos[\omega_s \tau + \varphi(t) - \varphi(t - \tau)].
\end{aligned} \tag{8}$$

To this point, photonic-assisted I/Q mixing is completed. In (7) and (8), the in-phase and quadrature parts of $\omega_s \tau + \varphi(t) - \varphi(t - \tau)$ are obtained with a common DC component (V_{DC}). To calculate the phase noise, V_{DC} should be acquired and removed. To do this, the 90° hybrid is replaced by a 180° hybrid to let the two driving signals applied to the DP-MZM be out of phase. In this case, the output voltages from PD1 and PD2, denoted by $v_7(t)$ and $v_8(t)$ respectively, are calculated to be

$$\begin{aligned}
v_7(t) &= V_{DC} + Q(t). \\
v_8(t) &= V_{DC} - Q(t).
\end{aligned} \tag{9}$$

If $v_7(t)$ and $v_8(t)$ are measured, V_{DC} can be known as

$$V_{DC} = \frac{v_7(t) + v_8(t)}{2}. \quad (10)$$

Once V_{DC} is known, the in-phase and quadrature components are obtained as

$$\begin{aligned} Q(t) &= v_5(t) - V_{DC} \\ I(t) &= v_6(t) - V_{DC} \end{aligned} \quad (11)$$

and the phase term $\omega_s \tau + \varphi(t) - \varphi(t - \tau)$ is

$$\theta(t) = \omega_s \tau + \varphi(t) - \varphi(t - \tau) = \tan^{-1} \left[\frac{Q(t)}{I(t)} \right]. \quad (12)$$

Based on (12), the power spectral density (PSD) of $\varphi(t) - \varphi(t - \tau)$ can be calculated by

$$\left[\varphi(t) - \varphi(t - \tau) \right]_{\text{PSD}} = S_{\theta}(f_m) = \left| \int_{-\infty}^{+\infty} \theta(t) e^{-j2\pi f_m t} dt \right|^2, \text{ for } f_m > 0. \quad (13)$$

where $S_{\theta}(f_m)$ is the PSD of $\theta(t)$. Finally, the single sideband phase noise of the UST can be obtained by [12]

$$L(f_m) = \frac{S_{\theta}(f_m)}{2|1 - e^{-j2\pi f_m \tau}|^2} = \frac{S_{\theta}(f_m)}{8\sin^2(\pi f_m \tau)}. \quad (14)$$

In practice, the signals in (7) and (9) should be sampled and digitized respectively using a two-channel analog-to-digital converter (ADC) before the phase noise is calculated according to (10)-(14). In the previous derivation, the laser phase noise is not considered. In fact, the two -1 st-order sidebands sent to PD1 or PD2 contain a common phase term related to the laser phase noise, which can be removed after photodetection. Therefore, the laser phase noise will not affect the measurement result. Besides, the system would not suffer from fiber dispersion induced RF power fading, because the optical signal sent to the PD contains only the -1 st-order sidebands. If there is slight difference between the amplitude responses of the in-phase and quadrature channels, e.g., the responsivities of the PD1 and PD2 are different, I/Q mismatch in amplitude would occur. This problem can be addressed by measuring the ratio between the response coefficients of the two channels in advance, and dividing the signal in one channel by this ratio.

Compared with the conventional frequency-discriminator-based systems, advantages of the proposed system are obvious. Firstly, the proposed system do not require feedback loop and tunable phase shifters. Therefore, the drawbacks due to the use of feedback loop (i.e., the system complexity and possible degradation of the measurement accuracy) are removed. Besides, the system applies photonic-assisted I/Q mixing using a 90-degree hybrid with a DP-MZM, which can have a large operation bandwidth and a compact structure compared to the system using pure electrical devices. In addition, optical fiber delay line is introduced to the phase noise measurement system based on quadrature phase demodulation, which can provide a large amount of delay and consequently helps to improve the measurement sensitivity.

3. Experimental demonstration

An experiment is carried out based on the setup shown in Fig. 1. The light from the LD (TeraXion, Inc., 1550.54 nm) is modulated by a PM (EOSPACE Inc.) which has a bandwidth of 40 GHz. A span of SMF with a length of 2 km is used to provide the time delay. The DP-

MZM (Fujitsu FTM7980EDA) has a 3-dB bandwidth of 22 GHz and a half-wave voltage of 1.8 V. The electrical 90° hybrid (Krytar, 3017360K) can work in the frequency from 1.7 GHz to 36 GHz. The optical spectrum after DP-MZM is measured by an optical spectrum analyzer (Yokogawa AQ6370C) with a resolution of 0.02 nm, as shown by the solid curve labeled with $E_3(t)$ in Fig. 2. After the DP-MZM, a frequency and bandwidth tunable OBPf (Yenista XTM-50) is applied to select out the -1st-order sidebands. Then, the optical signals in the two polarizations are separated using a PC and a PBS. The spectra of the two separated signals are also shown in Fig. 2 by the dash-dotted labeled with $E_{x2}(t)$ and the dashed curve labeled with $E_{y2}(t)$, respectively. After that, two 10 GHz PDs (Discoverysemi DSC50s) having the same parameters are used for optical-to-electrical conversions. The electrical signals after the PD are sampled by a two-channel 24-bit ADC (National Instruments PCIe-4462) with a sampling rate of 204.8 KSa/s. In the experiment, separating the x and y polarizations after the DP-MZM is a key step, which is easy to implement if polarization maintaining devices are used. Here, we provide another method to split the x and y polarizations. The PM is driven by a 10-GHz sinusoidal signal, and one RF port of the DP-MZM is driven by another sinusoidal signal at 10.1 GHz. A signal analyzer is used to monitor the spectrum of the electrical signal after PD1. Then, adjusting the PC before the PBS to a position where the electrical spectrum line at 100 MHz has a maximum power. In this way, the x and y polarizations of the optical signal after the DP-MZM can be separated. Another issue that should be noted is that, the 90° and 180° hybrid couplers should have a good phase balance to ensure an accurate measurement, because both the I/Q phase mismatch induced by the 90° hybrid and the DC voltage error caused by the 180° hybrid would result in phase noise measurement error.

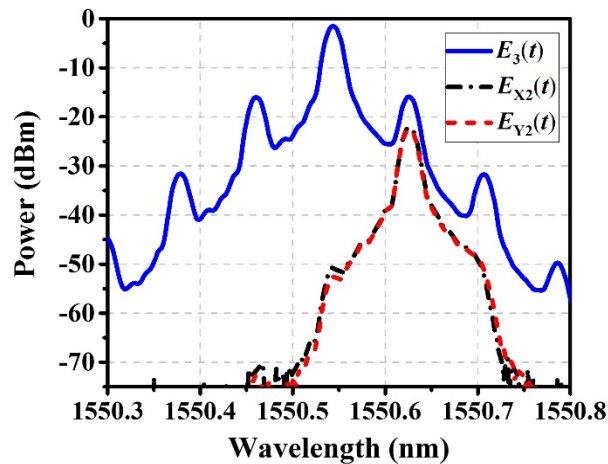


Fig. 2. The measured optical spectrum after the DP-MZM (blue solid curve) and the optical spectra of the selected -1st-order sidebands in the two polarizations (black dash-dotted curve and red dashed curve) when the frequency of the SUT is 10 GHz.

To check the measurement accuracy of the proposed system, the phase noise of a 10-GHz clock signal generated by a pulse pattern generator (Anritsu MP1763C) is measured with the result shown in Fig. 3. As a comparison, the phase noise measured by a commercial signal analyzer (R&S FSV40) is also included in Fig. 3. It is found that the two curves agree well with each other for offset frequency over 1 kHz. For offset frequency below 1 kHz, the phase noise measured by the established system is slightly higher than that measured by the commercial signal analyzer, which is mainly due to the fact that the coefficient of $1/[8\sin^2(\pi f_m \tau)]$ in (14) has an infinite response at zero offset frequency. The use of a longer fiber can help to get a more reliable phase noise at the low offset frequencies [14].

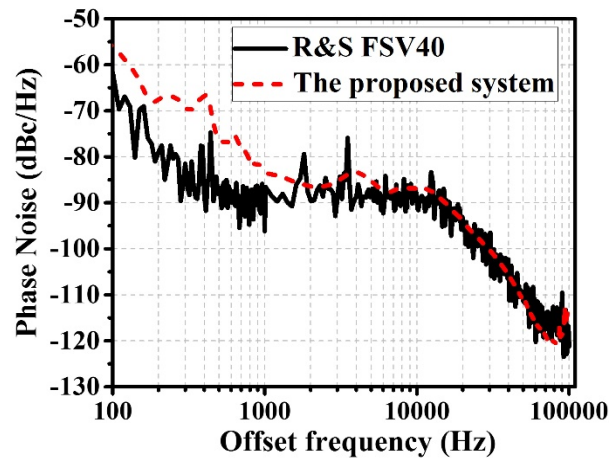


Fig. 3. Phase noise of a 10-GHz clock signal measured by the proposed system (red dashed curve) and by a commercial signal analyzer R&S FSV40 (black solid curve).

The phase noise measurement sensitivity can be evaluated by the phase noise floor, which refers to the minimum phase noise level that can be measured by the system. According to [10], by replacing the SMF with an attenuator that has the same attenuation with the SMF, the phase noise floor can be obtained. With this method, phase noise floor of the established system at 10 GHz frequency is measured and shown in Fig. 4(a). As can be seen, a low noise floor is achieved with -104 dBc/Hz and -131 dBc/Hz at 1 kHz and 10 kHz offset frequency, respectively. Considering the fact that there is an infinite response at around 107 kHz offset due to the coefficient of $1/[8\sin^2(\pi f_m \tau)]$ when using a 2-km SMF, the phase noise floor in Fig. 4(a) increases over 50.35 kHz offset. This is a common problem in photonic-delay-line based phase noise measurement systems that limits the reliable offset frequency range. When a longer fiber is applied as the delay line, the phase noise floor can be improved compared with the result in Fig. 4(a). However, the reliable offset frequency range would be reduced. This problem can be solved by applying a longer fiber for a close to carrier measurement and a shorter fiber for a far from carrier measurement [5]. Then, the phase noise of a 10-GHz signal generated by a microwave signal generator (Keysight E8257D-567) is measured by the proposed system and the commercial signal analyzer (R&S FSV40), respectively. The results are shown in Fig. 4(b), where several typical phase noises provided by the datasheet [15] are also included. As shown in Fig. 4(b), the phase noise measured by the proposed system is close to the values in the datasheet, indicating accurate phase noise measurement is achieved. However, because of the limited measurement sensitivity, the phase noise measured by the commercial signal analyzer is inaccurate for offset frequency over 1 kHz. This result not only confirms the measurement accuracy of the proposed system, but also verifies its good measurement sensitivity.

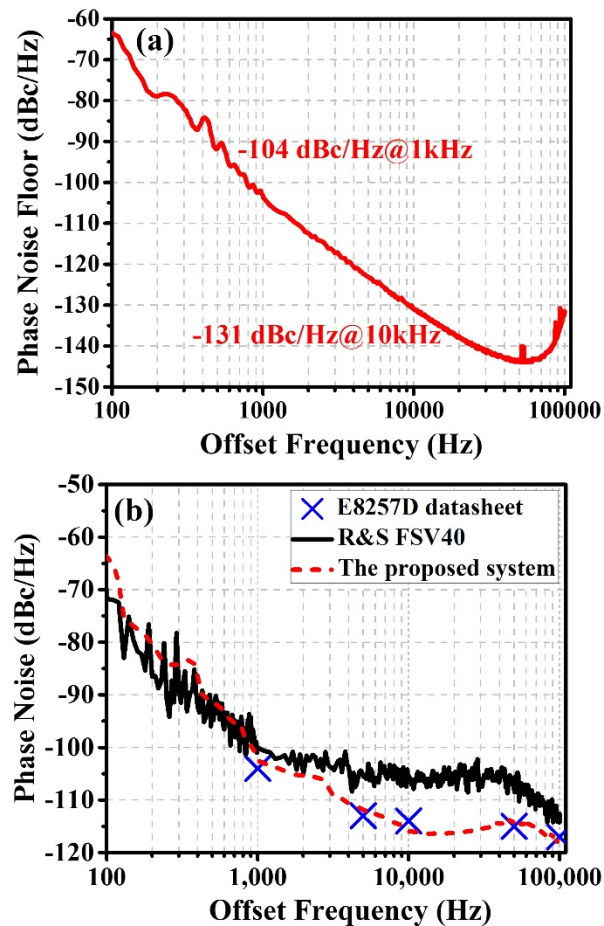


Fig. 4. (a) Phase noise floor of the established system at 10 GHz frequency, and (b) the phase noise of a 10-GHz signal from a microwave signal generator according, measured by the proposed system and by the signal analyzer R&S FSV40 (the blue marker are the values provided by the datasheet).

In addition to the good performance in measurement accuracy and sensitivity, another advantage of the proposed system is the large measurement frequency range because of the use of broadband optical fiber and photonic-assisted I/Q mixing. To demonstrate this property, phase noise of a frequency tunable single-frequency signal generated by the microwave signal generator (Keysight E8257D-567) is tested. The measured frequencies are from 5 to 35 GHz with a step of 5 GHz. Figure. 5 shows the measured phase noises at 10 kHz offset frequency for different frequencies. In Fig. 5, the typical phase noises provided by the datasheet are also included. It is found that the differences between the measured results and the typical values provided by the datasheet are kept within than 3 dB. This result can confirm that the proposed system can operate at a large frequency range from 5 to 35 GHz with a good measurement accuracy. In this demonstration, the lower limit of the measurement frequency range is determined by the edge slope of the tunable OBPF, which should be sharp enough to separate the -1 st-order sidebands from the optical carrier. The upper limit of the frequency range is determined by the operation bandwidth of the 90° hybrid as well as the bandwidth of the DP-MZM.

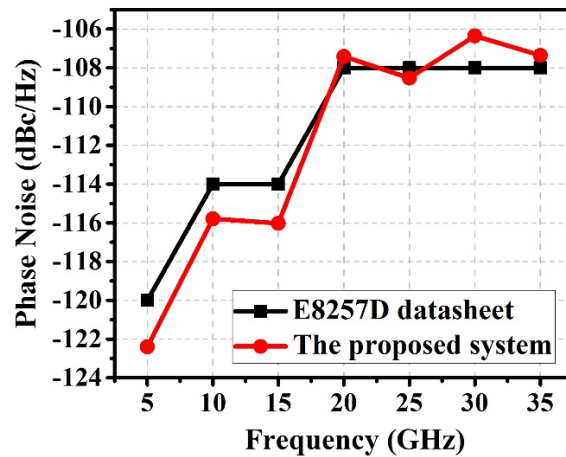


Fig. 5. Phase noises at offset frequency of 10 kHz of a wideband signal source (Keysight E8257D-567) measured by the proposed system (red-circle marker) and provided by the datasheet (black-square marker).

4. Conclusion

We have proposed and demonstrated a photonic-delay-line-based phase noise measurement system based on photonic-assisted I/Q mixing and digital phase demodulation. The prominent feature of the proposed system is that it can simultaneously achieve a high phase noise measurement sensitivity and a large measurement frequency range. In the experimental demonstration, accurate phase noise measurement is achieved in a large frequency range from 5 to 35 GHz. The phase noise floor of the measurement system applying a 2-km SMF is as low as -104 dBc/Hz@1 kHz and -131 dBc/Hz@10 kHz. These results can verify the good performance of the proposed system, which can be used for accurate phase noise measurement of wideband tunable microwave sources.

Funding

National Natural Science Foundation of China (NSFC) (61401201, 61422108); Natural Science Foundation Program of Jiangsu Province (BK20140822); Aviation Science Foundation of China (2015ZC52024); the open fund of Science and Technology on Monolithic Integrated Circuits and Modules Laboratory (20150C1404).